

RePose: A Real-Time 3D Human Pose Estimation and Biomechanical Analysis Framework for Rehabilitation

Junxiao Xue^{1†}, Pavel Smirnov¹, Ziao Li², Yunyun Shi³, Shi Chen³, Xinyi Yin⁴, Xiaohan Yue⁵, Lei Wang⁶, Yiduo Wang⁴, Feng Lin^{7,8}, Yijia Chen¹, Xiao Ma¹, Xiaoran Yan¹, Qing Zhang¹, Fengjian Xue³, Xuecheng Wu^{3,§}

¹Zhejiang Lab, ²Northeastern University, ³Xi'an Jiaotong University

⁴Zhengzhou University, ⁵Dalian Minzu University, ⁶Nanjing University of Aeronautics and Astronautics

⁷Fuyao University of Science and Technology, ⁸Xianghu Lab

[§]Corresponding author, [†]Project Lead

Abstract

We propose a real-time 3D human pose estimation and motion analysis method termed RePose for rehabilitation training. It is capable of real-time monitoring and evaluation of patients' motion during rehabilitation, providing immediate feedback and guidance to assist patients in executing rehabilitation exercises correctly. Firstly, we introduce a unified pipeline for end-to-end real-time human pose estimation and motion analysis using RGB video input from multiple cameras which can be applied to the field of rehabilitation training. The pipeline can help to monitor and correct patients' actions, thus aiding them in regaining muscle strength and motor functions. Secondly, we propose a fast tracking method for medical rehabilitation scenarios with multiple-person interference, which requires less than 1ms for tracking for a single frame. Additionally, we modify SmoothNet for real-time posture estimation, effectively reducing pose estimation errors and restoring the patient's true motion state, making it visually smoother. Finally, we use Unity platform for real-time monitoring and evaluation of patients' motion during rehabilitation, and to display the muscle stress conditions to assist patients with their rehabilitation training.

Date: January 5, 2026

Corresponding: xuecwu@gmail.com

1 Introduction

Whether for post-operative recovery or treatment of various musculoskeletal disorders, participating in physical therapy and rehabilitation plans are usually crucial. However, making a clinician available for every rehabilitation session is an impractical task and also economically unreasonable [21]. To address this issue, modern medical systems have begun adopting technologies and methods to provide remote monitoring and rehabilitation services. Remote monitoring, using sensors, mobile devices, and the internet, allows doctors to monitor patients' physiological indicators and rehabilitation progress in real-time, thus facilitating remote guidance and intervention. Such approaches can reduce the time patients stay in hospital and offer more convenient and cost-effective rehabilitation schemes.

Despite the development of various tools and devices to support physical rehabilitation, such as robot-assisted systems [22], virtual reality and gaming interfaces [7], and Kinect-based methods [16], there are still limitations in realizing a multi-functional and robust system for automatic monitoring and assessment of patient performance. Liao et al. [18]

introduced a deep learning framework for evaluating physical rehabilitation exercises, which assesses training through spatiotemporal modeling at multiple abstract levels. However, this method requires expensive optical motion capture systems for data acquisition. Swakhar et al. [4] proposed a method based on Graph Convolution Networks to evaluate physical rehabilitation exercises, offering self-attention of body joints, but still reliant on RGB-D cameras for input data. For the assessment of Parkinson's disease movement severity, Lu et al. [20] designed a posture-based evaluation system. Gu et al. [9] introduced an interactive computer vision system for home physical therapy that can track human movement and provide analysis, but lacks an assessment of specific muscle exertion levels. Although progress has been made, challenges remain in developing multi-functional and robust automatic monitoring and evaluation systems. To aid patients in receiving guidance and feedback in home physical therapy, an ideal support system needs to overcome two difficult challenges: firstly, the system must be capable to accurately analyze patient movements during exercises in real-time, which means it needs high-precision pose estimation capabilities to accurately capture joint angles and positions. Secondly, the system also needs to provide timely and specific feedback and guidance. This includes real-time suggestions and adjustments based on the patient's performance, as well as showing the correct posture and movement demonstrations to the patient. This helps patients to correct incorrect postures and ways of moving, ensuring they receive effective training and rehabilitation effects at home.

To overcome the aforementioned challenges, this paper proposes a method for real-time posture recognition in rehabilitation exercises, providing real-time feedback and guidance. This method is based on RGB video inputs and accurately estimates the patient's three-dimensional body position, enabling motion analysis and evaluation during exercise [43]. This method can be widely applied in various environments, such as analyzing human behavior in public places through surveillance cameras, or assisting individual rehabilitation training through smartphone cameras. By utilizing computer vision and deep learning techniques, our method has the following advantages. Firstly, it can monitor and evaluate the patient's rehabilitation behavior in real-time, providing immediate feedback and guidance to help the patient perform the exercise correctly. This is crucial for the effectiveness of the rehabilitation process, as it can help the patient correct incorrect movements, adjust postures, and enhance the exercise efficiency. Secondly, in experiments, we found that the range of motion for patients in rehabilitation scenarios is relatively smaller compared to healthy individuals, resulting in noticeable jitters in the reconstructed body model. To address this issue, we utilize the SmoothNet [45] to reduce jitters. This filter can make the reconstructed body model smoother and more realistic, improving the accuracy and reliability of posture recognition. Furthermore, in rehabilitation scenarios with multiple participants (such as family members, doctors, etc.), the model only tracks and detects the behavior and movements of a specific individual rehabilitation patient. This helps focus on analyzing and evaluating the specific patient's rehabilitation progress, providing personalized rehabilitation plans and support. Finally, we utilize the Unity platform to visually demonstrate muscle and skeletal forces. By creating virtual environments and presenting them in three-dimensional forms, we can visualize the forces on muscles and skeletons during the rehabilitation process, enhancing the effectiveness and quality of the rehabilitation treatment experience.

To overcome the aforementioned challenges, this paper proposes a real-time posture recognition method for rehabilitation exercises that provides immediate feedback and guidance. Based on RGB images or video input, this method can accurately estimate the patient's three-dimensional body position, enabling the analysis and assessment of actions during the movement process. This method can be widely applied in various environments, such as analyzing human behavior in public places through surveillance cameras, or assisting personal rehabilitation training through smartphone cameras. By using computer vision and deep learning technologies [37, 40], our method has the following advantages. Firstly, it can monitor and evaluate the patient's rehabilitation behavior in real-time, providing immediate feedback and guidance, helping patients perform movements correctly. This is vital for the effectiveness of the rehabilitation process, helping patients correct errors promptly, adjust posture, and enhance exercise effects. Secondly, we integrated SmoothNet into pipeline to reduce jitters. It can lower high-frequency components in the data, making the reconstructed human model more stable, thus enhancing the accuracy and reliability of posture recognition. Thirdly, in rehabilitation scenarios with multiple participants (such as family members, doctors, etc.), the model only tracks and detects the behavior and actions of a rehabilitation patient. This helps concentrate efforts on analyzing and evaluating the specific patient's rehabilitation progress, providing personalized rehabilitation plans and support [42]. Finally, we leverage the Unity platform to visually demonstrate the muscular and skeletal stresses. Through the creation of a virtual environment and its three-dimensional representation, we are able to visually display the forces exerted on the musculoskeletal system during rehabilitation, thus enhancing the effectiveness and quality of the therapeutic experience.

In conclusion, the main contributions of this paper are as follows:

- We propose RePose, a real-time human pose estimation pipeline that maintains approximately 30 FPS on a Linux system in a multi-person medical rehabilitation scenario and is also capable of running on a Windows system.
- In the presence of multiple participants, our model exclusively tracks and detects the movements and actions of a specific individual undergoing rehabilitation. Additionally, a SmoothNet is utilized to reduce jitters caused by errors in pose estimation.
- By utilizing the Unity platform, we facilitate intuitive and real-time monitoring and assessment of rehabilitation behaviors and exhibit the muscular and skeletal stress conditions to assist patients in their rehabilitation training and therapy.

The organization of the paper is as follows: Section 2 provides an overview of related work. Section 3 introduces the proposed real-time rehabilitation exercise pose recognition framework and musculoskeletal stress analysis. Section 4 presents the validation of the proposed RePose framework on a public dataset. Section 5 proposes several promising directions for future research. Lastly, Section 6 concludes the paper.

2 Related Work

2.1 Human Pose Estimation

Human Pose Estimation constitutes the process of locating human body parts and constructing human representations, such as the skeletal structure [50], from input data including images or videos. Human Pose Estimation (HPE) provides quantitative information regarding human motion, which can be utilized by medical professionals to diagnose complex conditions, create rehabilitative training programs, and guide physical therapy.

Object Detection. For a comprehensive image understanding, it is essential not just to classify different images but also to estimate the concepts and locations of objects contained within each image. General object detection aims to locate and classify objects present in any given image, primarily falling into two categories: one that follows the traditional object detection workflow, initially generating region proposals and then classifying each proposal into different object categories. The other views object detection as a regression or classification problem, adopting a unified framework to directly produce final results (both category and location) [49]. Region proposal-based methods such as Fast R-CNN [8], Faster R-CNN [28], Feature Pyramid Networks (FPN) [19], and Mask R-CNN [12] generate region proposals followed by object classification and localization based on these proposals. On the other hand, the regression/classification-based methods have adopted different object detection methodologies. They regard object detection as a regression or classification challenge, aiming to predict an object’s category and location directly without depending on region proposals. The regression/classification-based methods include Deconvolutional Single Shot Detector (DSSD) [6], Deeply Supervised Object Detectors (DSOD) [29], YOLOv5 [39], and YOLOv8 [33]. These methods typically extract features from input images using deep neural networks and employ various techniques (such as Anchor boxes) to predict the categories and bounding box coordinates of objects. While region proposal-based methods achieve high precision at a significant computational cost, regression/classification-based methods prioritize real-time processing at the expense of some accuracy.

2D Human Pose Estimation. The methodology of 2D Human Pose Estimation (2D HPE) involves estimating the two-dimensional spatial location of human body keypoints from images or video sequences. Depending on the number of subjects in the image, this can be categorized into two distinct approaches: single-person pose estimation and multi-person pose estimation [41]. Single-person pose estimation is a foundational research area within 2D HPE that does not require consideration of occlusions between targets. In general, single-person pose estimation can be approached via regression methods or heatmap-based methods. Regression methods employ an end-to-end framework to learn the mapping from input images to the positions of body joints or parameters of a human body model. By training a deep neural network, regression methods are capable of predicting the precise locations of body joints directly from images. For instance, the DeepPose method by Toshev et al. [34] tackles the problem of body joint regression based on Deep Neural Networks (DNNs). Sun et al. [32] introduced “Compositional Pose Regression,” a structure-aware regression method based on ResNet-50, utilizing a reparameterized pose representation that substitutes joints with bones. The advantage of these methods lies in their ability to estimate the positions of multiple joints simultaneously and to handle variations in human body shapes and postures. Another prevalent approach is the heatmap-based method. This approach aims to predict the approximate locations of body parts and joints, supervised by their representations on heatmaps [38].

Specifically, heatmap-based HPE methods estimate 2D heatmaps instead of directly estimating the two-dimensional coordinates of body joints by placing 2D Gaussian kernels at each joint’s location. Heatmaps are two-dimensional matrices of the same size as the image, where each element indicates the confidence level for the corresponding body part or joint. By training a deep neural network, heatmap-based methods are able to generate heatmaps from the input image and extract positional information of keypoints from them. For example, Newell et al. [23] proposed the “Stacked Hourglass” encoder-decoder network that performs iterative bottom-up and top-down processing with intermediate supervision. Sun et al. [31] introduced a High-Resolution Net (HRNet) that acquires more accurate keypoint heatmap predictions by learning reliable high-resolution representations through the parallel connection of multi-resolution subnetworks and repeated multi-scale fusions.

3D Human Pose Estimation. The objective of 3D Human Pose Estimation (3D HPE) is to predict the position of human body joints within three-dimensional space. The aim of 3D HPE is to accurately estimate the three-dimensional coordinates of the human body’s joints from a given input, such as an image or video sequence. This process necessitates an understanding of the spatial relationships between different body parts and inferring their positions within the three-dimensional world. Precise estimation of 3D human pose can provide valuable information about body mechanics, which can be utilized in various applications including motion analysis, rehabilitation, and animation. Approaches to 3D HPE can be generally categorized into two types: model-based and model-free. Model-based methods utilize prior knowledge about human anatomy and kinematics to reconstruct a three-dimensional posture, typically by fitting a parametric human body model to the input data and optimizing its parameters to align with observed joint positions. On the other hand, model-free methods employ deep learning techniques to directly regress the three-dimensional joint positions from input data, without explicitly relying on a predefined human body model. Based on the number of views and the number of individuals in the scene, 3D HPE methods are subdivided into three categories: single-view single-person 3D HPE, single-view multi-person 3D HPE, and multi-view 3D HPE. In this paper we primarily investigate multi-view and model-free methods. Iskakov et al. [24] proposed a multi-view 3D human pose estimation scheme based on a learnable triangulation method. Zhang et al. [47] introduced AdaFuse, which aggregates 2D keypoint heatmaps from multi-view images into a three-dimensional structural model, based on all camera parameters after calibration. Tu et al. [35] presented VoxelPose, which aggregates features from each camera view in a 3D voxel space. They designed a cuboid proposal network and a pose regression network to localize all individuals and estimate their 3D poses, respectively. Zhang et al. [46] proposed the Multi-view Pose transformer (MvP), a model that regresses 3D poses directly from multi-view images without reliance on any intermediary tasks. To reduce the computational cost of VoxelPose, Ye et al. put forward Faster VoxelPose [44], which reprojects the feature volume onto three two-dimensional coordinate planes and estimates the X, Y, and Z coordinates separately, thereby increasing the speed of VoxelPose by a factor of ten.

2.2 Musculoskeletal Movement forces

Human movement is driven and supported by the musculoskeletal system, which includes bones, skeletal muscles, joints, and soft connective tissues, together forming a complex multi-body system [36]. To address the motion issues within musculoskeletal models, both forward and inverse solutions are typically employed. Forward kinematics approaches take electromyography (EMG) measurements [10, 27] or neural commands obtained from controllers [11, 26] as model inputs to predict the motion state of the human body. This method can be used to estimate the intensity and timing of muscle activities, thereby inferring the body’s posture and movement. However, forward kinematics approaches are relatively computationally inefficient and challenging to apply to complex motion studies such as three-dimensional gait analysis. In contrast, inverse kinematics approaches use measured joint kinematics and external forces as model inputs to estimate joint torques and muscle forces [25, 30]. This method infers muscle activation patterns and force outputs by back-calculating muscle torques and joint forces, and is significantly valuable in studying human motion control and rehabilitation therapy.

2.3 Rehabilitation Systems

Various home-use devices for rehabilitation have been developed, including robots, wearable devices, and Kinect-based rehabilitation applications. Robotic rehabilitation [5] devices can assist patients in their rehabilitation exercises through the robot’s strength and precision. These devices often feature multiple joints and sensors to offer personalized rehabilitation therapy. For instance, lower-limb rehabilitation robots like Lokomat, Hocoma, and others, utilize principles of extracorporeal therapy by supporting the patient’s lower limb movements to facilitate the rehabilitation of lower limb dysfunctions. Robotic rehabilitation devices provide highly accurate motion control, which can precisely monitor

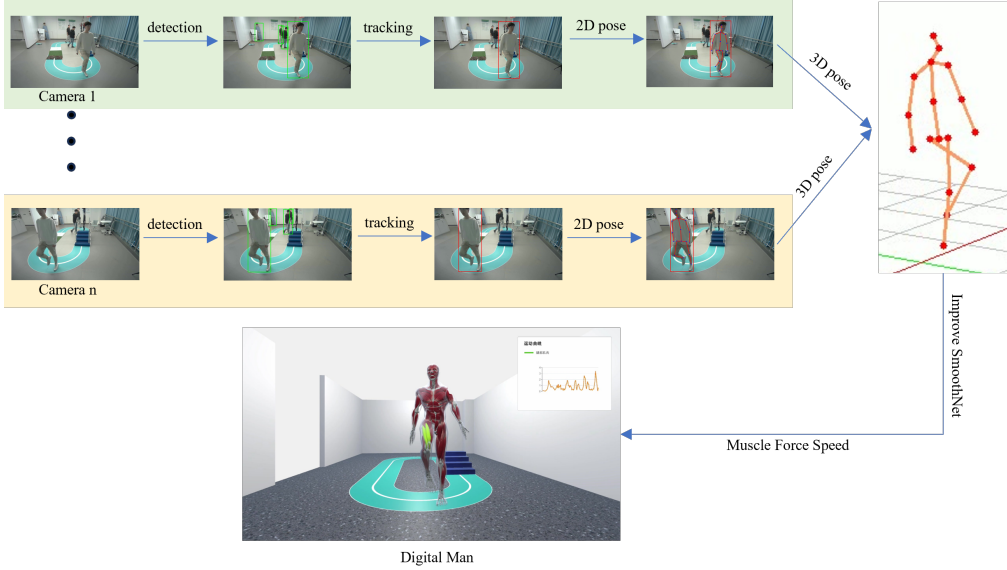


Figure 1 Overview of introduced RePose multi-camera real-time digital human pipeline. The red box represents the tracking box. Each camera generates a 2D pose and synthesize a 3D pose. And then generates to digital human.

and correct patients' actions, thereby aiding in the recovery of muscle strength and motor function. However, these robots [2, 15] are costly, bulky, and only offer specific types of rehabilitation training. Wearable devices are directly worn on the body to monitor and assist the patient's movements. These devices are compact and portable, allowing patients to wear them at any time and place for rehabilitation exercises. Nonetheless, wearable devices usually only monitor and support specific parts or types of movement. For whole-body movements or rehabilitation involving multiple joints, additional equipment or methods may be required. Kinect-based rehabilitation applications utilize the Microsoft Kinect sensor for rehabilitation training. Kinect-based applications do not require direct patient contact with the device and can support various types of rehabilitation exercises by using the camera to identify and track the patient's movements. However, due to the limitations of camera technology, they may not provide highly accurate motion tracking and control, and the purchase of Kinect-specific hardware is necessary.

3 Method

Solution Framework. Our approach reconstructs a 3D virtual digital human body model from multiple video streams. Prior to 3D HPE, it is necessary to calibrate the intrinsic and extrinsic parameters of the cameras used to acquire the mapping relationship between the 2D image coordinate system and the 3D spatial coordinate system. This calibration allows to convert detected human 2D coordinates into 3D coordinates. Subsequently, multi-camera system capture multiple synchronous video streams, and the following processing steps are applied to each frame of each video stream. The YOLO-v5 [39] object detection model is employed to estimate the position and output bounding boxes of people in video. After that, tracking algorithm is applied to track the person whose pose should be estimated. For the multi-view 3D pose estimation, we follow the approach proposed in [14]. We crop an image of the person of interest using tracked bounding box and estimate the positions of 17 human body joints for each frame. Based on the 2D coordinates of the 17 detected joints in multiple image frames at the same timestamp, the positions of the corresponding joints in 3D space are estimated using the learnable linear triangulation method. Next, we use SmoothNet to filter the 3d joint positions and feed them into the digital human part for musculoskeletal calculations. The process flow is illustrated in Figure 1.

3.1 Human Pose Estimation Model

Object Detection. In the object detection phase, OpenCV library is utilized to read video streams from cameras, and pretrained YOLOv5 model to detect people. Briefly the process can be described as follows. Firstly, the backbone network extracts features from the input image; then, the feature fusion module outputs feature maps of different scales;

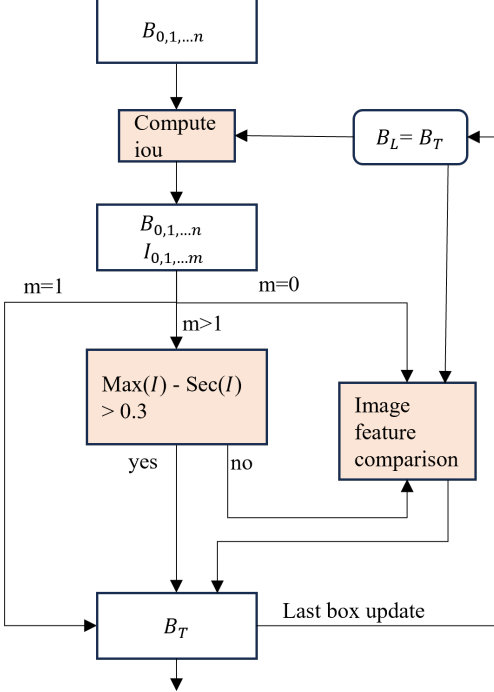


Figure 2 Flowchart of the proposed real-time single-person tracking algorithm with hierarchical decision logic designed for complex multi-person rehabilitation scenarios.

finally, the prediction module outputs regression parameters for target boundary boxes and target categories based on the feature maps. Identified human figures are extracted by setting non-maximum suppression (NMS).

Object Tracking. In actual rehabilitation scenarios, it is common to have situations where either an individual or multiple people are present simultaneously. Here, an individual refers to the patient whose pose should be estimated and multiple people can include the patient, family members, and medical personnel. In such scenarios, it is necessary to track the patient in order to better monitor and assist the rehabilitation process. When there is only a single person present, that is, $n=1$, real-time individual tracking is conducted directly. However, if multiple human figures are detected, resulting in n bounding boxes $B_{boxes} = [B_0, B_1 \dots B_n]$, that is, $n>1$, it becomes necessary to employ a tracking algorithm to focus specifically on the rehabilitation control and assessment of the patient.

As shown in Figure 2 above, we employ the similarity calculation based on the Intersection over Union (IoU) to measure the degree of overlap between two bounding boxes. The larger the overlapping area, the larger the value of IoU. Specifically, first we save the target box B_L of the previous frame as the tracking object, and then calculate its IoU with all the boxes in the current frame B_{boxes} . If the IoU is greater than a certain threshold (default value is 0.2), the B_i is considered a candidate box, and the number of candidate boxes is m ($m \leq n$). If $m=1$, the current candidate box is considered to be the best tracking target B_T . If $m>1$, we sort the candidate boxes and calculate the difference between B_{boxes} with highest values of IoU and if the difference is greater than or equal to 0.3, the B_{boxes} with the largest value of IoU is considered to be the best tracking target B_T . Otherwise (or for $m=0$), indicating that the tracking box B_T cannot be accurately located solely based on IoU, some other image feature extraction methods are used to estimate similarity of detected B_{boxes} for the current frame and tracked B_{boxes} from the previous frame. Specifically, the color features of the candidate n B_{boxes} are calculated, and the same method is applied to the B_L . Then, feature similarity between each candidate B_{boxes} and the B_L is estimated one by one and the bounding box with the highest value of feature similarity is chosen as the tracking object B_T .

Although other existing solutions for tracking can provide higher accuracy, they would require more computational resources. However in the actual medical rehabilitation scenarios, there is generally no overlap between the patient and the surrounding people, such as, m is generally equal to 1. For such case our tracking algorithm does not require feature calculations, it only relies on IOUs comparison, which results in high processing speed and high accuracy. As shown in

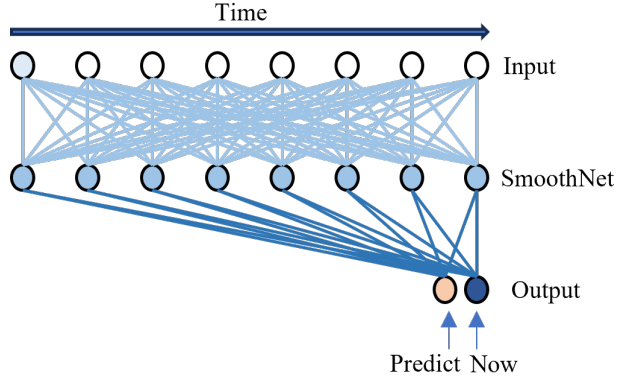


Figure 3 Architecture of the modified SmoothNet for real-time temporal refinement and motion prediction.

Table 1, the average inference time of our tracking algorithm takes less than 1 millisecond.

2D Pose Estimation. Our pose estimation algorithm follows the approach proposed in [14]. Initially, we use the bounding box Bbox to crop the image of the patient I_c . Subsequently, 2D pose estimation backbone ResNet152 takes this image as an input to estimate joint heatmaps $H_{c,j} = h_\theta(I_c)_j$, where $H_{c,j}$ represents the heatmap for joint j in image I_c , h_θ denotes a 1×1 convolution kernel, $j \in 1, \dots, J$, and J is the number of joints. To estimate the 2D positions based on the joint heatmaps, we first compute the softmax along the spatial domain of the heatmap as follows:

$$H'_{c,j} = \frac{\exp(\alpha H_{c,j})}{\sum_{r_x=1}^W \sum_{r_y=1}^H \exp(\alpha H_{c,j}(r))} \quad (1)$$

Here, $H'_{c,j}$ indicates the heatmap after applying the softmax operation, W and H respectively denote the width and height of the heatmap, $H_{c,j} = h_\theta(I_c)_j$ refers to the heatmap value at coordinates r , and α is a hyperparameter that adjusts the heatmap. The central position for each joint in 2D is calculated using the soft-argmax operation on the heatmap $H'_{c,j}$:

$$x_{c,j} = \sum_{r_x=1}^W \sum_{r_y=1}^H r \cdot (H'_{c,j}(r)), \quad (2)$$

where $x_{c,j} \in R^{J^2}$ denotes the two-dimensional coordinates corresponding to the joint points in the heatmap $H'_{c,j}(r)$, thereby obtaining the two-dimensional coordinates of all joint points in each view.

3D pose estimation. After obtaining the two-dimensional joint positions $x_{c,j}$ in the image, we infer the three-dimensional positions of the joints y_j using linear algebra triangulation. To facilitate computation, the problem of computing three-dimensional coordinates is reduced to solving an overdetermined system of equations on the homogeneous three-dimensional coordinate vector:

$$(w_j \circ A_j) y_j = 0. \quad (3)$$

Here, y_j represents the sought three-dimensional coordinate vector, $A_j \in R^{2C^4}$ is a matrix composed of the projection matrix P_C and the two-dimensional joint coordinates $x_{c,j}$. w_j is estimated by the convolutional network q_ϕ , with inputs from the output of the ResNet152 network, where \circ denotes the Hadamard product. Finally, the three-dimensional positions of the joints y_j are solved using Singular Value Decomposition (SVD).

Modify SmoothNet. To attain smoother 3D pose estimations and achieve higher frames per second (FPS), we have refined the SmoothNet [45] algorithm for real-time 3D pose estimation. The original SmoothNet algorithm is only applicable to video data, requiring temporal information not only from current and previous frames but future frames as well. However for real-time processing only historical data is available. Furthermore, our goal was also to enhance the visual coherence of outputs through interpolation of estimated poses between frames, thereby increasing the FPS. The model architecture follows the original SmoothNet, with modifications to the input and output data as well as the training



Figure 4 The musculoskeletal digital human model used for muscle stress quantification and visualization.

loss. Figure 3 illustrates the schematic of the Modify SmoothNet algorithm. In the Modify model, we input the 3D poses of the current and preceding eight frames, enabling the model to output poses for two frames, the current frame and the predicted intermediate frame. This design allows us to double the FPS for smoother visualization.

Moreover, beyond using position loss, we have incorporated velocity loss to ensure a smoother output of poses. We use velocity loss since we output only two joint points, i.e., the current frame and the predicted frame. The training loss (Loss) function is computed as:

$$L_{total} = \alpha L_{pos} + (1 - \alpha) L_{acc}, \quad (4)$$

$$L_{pos} = \frac{1}{T \times C} \sum_{t=0}^T \sum_{i=0}^C |G_{t,i} - Y_{t,i}|, \quad (5)$$

$$L_{vel} = \frac{1}{T \times C} \sum_{t=0}^T \sum_{i=0}^C |G_{t,i} - G_{t-1,i}| |Y_{t,i} - Y_{t-1,i}|. \quad (6)$$

Here, α denotes the proportionality coefficient between the two losses, T and C represent the number of output time frames and output joints, respectively, $G_{t,i}$ and $Y_{t,i}$ represent the ground truth joint positions and the estimated joint positions, while $|G_{t,i} - G_{t-1,i}|$ and $|Y_{t,i} - Y_{t-1,i}|$ signify the velocity of joint i at time frame t .

3.2 Calculate muscle forces

Calculation of muscle stress quantification. The world coordinates derived from the above models are based on a right-handed coordinate system, whereas Unity commonly employs a left-handed coordinate system. Consequently, we first transform the three-dimensional coordinate system using the Rodrigues' rotation formula to align the origin and axes with those of Unity's coordinate system. Subsequently, we utilize the FABRIK (Forward And Backward Reaching Inverse Kinematics) algorithm [1] to achieve inverse kinematics. Given the received coordinate data as input for target points, we drive the motion of a digital human model through the FABRIK algorithm, which calculates the positions and poses of the model's joints based on the target point location and constraint conditions. We employ an original digital human model obtained from the Unity library, as depicted in Figure 4. By adjusting the digital human model's pose frame-by-frame, we ensure it aligns with the target points.

The FABRIK algorithm is based on the iterative solving approach, which approximates the target point through multiple



Figure 5 Color-coded heatmap representation for muscle stress visualization during rehabilitation exercises.

iterations. The input consists of the target position t and the distances between each joint position

$$d_i = |p_{i+1} - p_i|, \quad (7)$$

where p_i represents the joint position coordinates, $i=1, \dots, n-1$. The final joint positions p_i are computed by iterating the algorithm.

Assuming p_1 is the root joint, the distance between the root joint and the target position is given by

$$dist = |p_1 - t|. \quad (8)$$

If $dist > d_1 + d_2 + \dots + d_{n-1}$, then the target position is unreachable. In this case, the distance between the target position and the joint positions r_i is determined using the following formula:

$$r_i = |t - p_i|, \quad (9)$$

$$\lambda_i = \frac{d_i}{r_i}. \quad (10)$$

The new joint position P_{i+1} is determined as:

$$p_{i+1} = (1 - l_i)p_i + l_{it}. \quad (11)$$

If $dist \leq d_1 + d_2 + \dots + d_{n-1}$, then the target position is reachable. Assuming the initial position of the root joint p_1 is b , we first check if the distance between the end effector p_n and the target t is greater than a tolerance value tol

$$dif_A = |p_n - t|. \quad (12)$$

If $dif_A > tol$, we perform forward reaching by setting the end effector p_n to the target position t , i.e., $p_n = t$. The distance between the target and joint positions r_i is computed as:

$$r_i = |p_{i+1} - p_i|, \quad (13)$$

$$\lambda_i = \frac{d_i}{r_i}. \quad (14)$$

The new joint position p_i is determined as:

$$p_i = (1 - l_i)p_{i+1} + l_i p_i. \quad (15)$$

Next, we perform backward reaching by setting the root joint p_1 to the initial position $p_1 = b$. The distance between the new joint positions r_i is computed as:

$$r_i = |p_{i+1} - p_i|, \quad (16)$$

$$\lambda_i = \frac{d_i}{r_i}. \quad (17)$$

The final joint position is determined as:

$$p_{i+1} = (1 - \lambda_i)p_i + \lambda_i p_{i+1}. \quad (18)$$

Throughout the algorithm's execution, FABRIK initiates by setting the initial joint positions of the digital human model. Subsequently, it iteratively adjusts the positions of the joints to bring the extremities of the digital human model, such as the hands or feet, as close as possible to the target point. Concurrently, the FABRIK algorithm adheres to the joint constraints, ensuring the digital human model's posture remains within physiological limits. This method allows for precise control over the digital human model, enabling it to move in response to the target data received.

Muscle Force Speed. The calculation of muscle force typically involves the measurement of changes in velocity. When muscles are subjected to external forces or their own contraction, they generate movement, which, in turn, causes changes in velocity at related skeletal joints. By measuring the changes in velocity, we can infer the state of muscle force. Initially, it is essential to determine the correlation between muscle mesh skinning and skeletal joints. For instance, based on anatomical data, the triceps brachii are located on the posterior side of the arm, acting on the shoulder joint and forearm, and antagonizing the biceps brachii. Utilizing Unity software, one can identify the skeletal joints associated with the triceps brachii and use the velocity of these joints to deduce the muscle's force generation. Subsequently, the motion velocity of the skeletal joints is computed. At every frame update, the three-dimensional vector of the current frame is subtracted from that of the previous frame, and then divide it by the frame time difference (0.02f), resulting in a three-dimensional vector representing the velocity of the skeletal node, defined as:

$$V = \frac{(x_n, y_n, z_n) - (x_{n-1}, y_{n-1}, z_{n-1})}{0.02f}. \quad (19)$$

Using coroutines allows for the continuous calculation of the joint's velocity vector. Since coroutines operate in the background, they can perform continuous calculations and updates without blocking the main thread during frame-by-frame execution. Finally, the muscle's color is adjusted in real-time based on changes in the skeletal motion velocity. The absolute value of the velocity vector is obtained and weighted on the x, y, and z axes to estimate the muscle's force intensity. This intensity is classified into three levels: intense, moderate, and slow, with thresholds defined as "speed". An intensity level is considered intense if "speed" is equal to or greater than 0.2, moderate if "speed" is less than 0.2 but greater than 0.08, and slow if "speed" is equal to or less than 0.08. These intensity levels are visually represented on the corresponding muscle mesh skinning using yellow, green, and blue colors, respectively.

4 Experiment

4.1 Datasets and Evaluation Metric

We adopt the most commonly used evaluation protocols. Protocol 1 is the Mean Per Joint Position Error (MPJPE) which measures the mean Euclidean distance between the ground truth and estimated joints in millimeters. The MPJPE formula is defined as:

$$E_{\text{MPJPE}}(f, S) = \frac{1}{N_S} \sum_{i=1}^{N_S} \left\| P_{f,S}^{(f)}(i) - P_{\text{gt},S}^{(f)}(i) \right\|_2, \quad (20)$$

where f denotes a frame and S denotes the corresponding skeleton. $P_{f,S}^{(f)}(i)$ is the estimated position of joint i and $P_{\text{gt},S}^{(f)}(i)$ is the corresponding ground truth position. All joints are considered, $N_S = 17$. The MPJPE are averaged over all frames. Protocol 2 is the MPJPE after aligning the predicted 3D pose with the ground truth using translation, rotation, and scale (P-MPJPE).

Table 1 Real-time pipeline inference speed. “Prep in detection” refers to the image transformation prior to target detection, “prep in 3d pose” pertains to image cropping preceding the 3D segment, and “W/O or W in Fps” signifies whether fps is doubled through SmoothNet.

Num cam	Video	Detection		Track	3D Pose			Total (ms)	FPS	
		Prep	YOLO		Prep	2D	3D		W/O SN	W SN
4	Offline	9.1	2.1	2.5	9.3	6.0	1.7	30.7	33	66
2	Offline	4.4	1.3	1.9	4.8	2.9	1.4	16.7	60	120
4	Online	25.0	2.7	2.1	13.2	5.7	4.9	53.6	19	38
2	Online	22.5	2.0	1.4	7.0	3.8	4.0	40.7	25	50

Table 2 Quantitative comparison with the state-of-the-art methods on Human3.6M under Protocol 1. * means the ground truth bounding boxes provided by the dataset, † means bounding boxes with our proposed detection and tracking algorithm.

Methods	VideoPose3D* [24]	Anatomy3D* [3]	MHFormer* [17]	PoseFormerV2* [48]	Pipeline4† (Ours)
Dir.	45.16	41.49	39.17	41.26	25.61
Dis.	46.67	43.80	43.06	45.45	33.44
Eat	43.31	39.77	40.07	41.47	35.51
Gre.	45.61	43.12	40.94	44.04	31.47
Phon.	48.10	46.18	44.95	46.67	63.73
Pho.	55.13	52.54	51.16	53.75	28.62
Pose	44.62	42.16	40.63	42.63	25.44
Pur.	44.28	41.85	41.29	42.64	29.68
Sit	57.30	54.15	53.56	55.19	137.46
SitD.	65.79	60.70	60.37	64.62	111.77
Sm.	47.09	45.49	43.71	45.71	46.28
Wait	43.99	41.56	42.12	42.89	26.70
WD.	48.96	46.04	43.84	45.76	30.67
Walk	32.80	31.41	29.76	32.34	27.72
WT.	33.89	32.45	30.59	32.89	26.24
Avg.	46.85	44.18	42.95	45.15	45.36

To validate the accuracy and real-time performance of our modeling framework, we conduct validation tests at the Human3.6 Dataset [13]. The Human3.6 Dataset have 4 high-resolution progressive scan cameras to acquire video data at 50 Hz. The dataset consists of 11 different human movement categories covering a wide range of movements in daily life, such as walking, running, lifting weights, etc. Each movement category has several different instances of human motion captured from different angles and views. Following previous works, we train a single model on five subjects (S1, S5, S6, S7, S8) and test it on two subjects (S9 and S11).

4.2 Implementation Details

Our pipeline is implemented on PyTorch. During training, for the 2D pose estimation network, we adhere to the setup as prescribed in [14]. For YOLO-v5m, we employ the pre-trained data provided by the official source. For SmoothNet, we follow the training configuration detailed in [45], utilizing the human3.6 dataset for training purposes. Regarding model deployment, pipeline inference is conducted on a Linux server, while visualization is carried out on a Windows server utilizing the Unity platform. Notably, for the YOLO and 2D model components, we convert them into 16-bit floating-point type to diminish model weight, and employ TensorRT for model acceleration.

Table 1 documents the number of different cameras utilized by our model as well as the inference speeds in video testing and real-time scenarios. It is evident that our pipeline delivers commendable real-time performance. “Num cam” refers to the number of cameras employed, “video” denotes whether the input data is “offline or online”, indicative of real-time

Table 3 Quantitative comparison with the state-of-the-art methods on Human3.6M under Protocol 2.

Methods	VideoPose3D* [24]	Anatomy3D* [3]	MHFormer* [17]	PoseFormerV2* [48]	Pipeline† (Ours)
Dir.	34.12	33.01	31.36	32.34	23.38
Dis.	36.12	35.29	34.91	35.87	31.27
Eat	34.43	32.63	32.81	33.78	37.66
Gre.	37.22	35.37	33.85	35.81	23.93
Phon.	36.39	35.85	35.32	35.97	47.75
Pho.	42.20	40.43	39.63	41.13	25.59
Pose	34.42	32.86	31.92	33.17	23.35
Pur.	33.59	32.50	32.22	32.71	26.43
Sit	45.03	42.33	43.56	44.26	58.61
SitD.	52.53	49.69	48.96	51.93	50.29
Sm.	37.37	36.88	36.36	37.42	39.72
Wait	33.80	32.47	32.58	32.84	24.73
WD.	37.75	36.13	34.42	35.58	27.81
Walk	25.64	25.02	23.85	25.23	25.22
WT.	27.80	26.34	25.10	26.56	23.93
Avg.	36.53	35.12	34.48	35.64	32.64

processing. “Prep in detection” refers to the image transformation prior to target detection, “prep in 3d pose” pertains to image cropping preceding the 3D segment, and “W/O or W in Fps” signifies whether fps is doubled through SmoothNet. The rationale for offline being faster than online is attributed to the considerable time and computational resources required for camera reading.

4.3 Main Results

We have tested and report the accuracy of our pipeline on the human3.6 dataset. Although our principal innovation is not in pose estimation, our pipeline still demonstrates impressive performance. As illustrated in Tables 2 and 3, where * signifies the utilization of ground truth detection boxes provided by human3.6. “Pipeline” denotes inference using an end-to-end approach, and † signifies the employment of our in-house developed object detection and tracking algorithm, accelerated through TensorRT, as well as the lightweight 16-bit floating-point model described in Section 4.2. Even without the use of ground truth detection boxes from human3.6, our pipeline exhibits performance comparable to current advanced models under Protocol 1 standards. Under the evaluation criteria of Protocol 2, our pipeline even achieves the best outcomes. This indicates that our pipeline maintains model accuracy while ensuring inference speed, thus validating the effectiveness and practicality of our approach.

4.4 Visualization

To demonstrate the efficacy and versatility of our pipeline, we have presented its application in real-world scenarios as shown in Figure 6. At the initial stage of the original image, we display only the perspective of the first camera. Following the object detection, object tracking, and 2D pose estimation modules, we obtained the 2D keypoints. Subsequently, by processing these 2D keypoints from multiple cameras through the 3D pose estimation and the Improved SmoothNet modules, we acquired the 3D keypoints. Ultimately, through the Calculation of Muscle Stress Quantification and Muscle Force Speed computations, we derived the displayed digital human. In practice, the muscle changes in the digital human can be dynamically displayed in real-time through color and motion trajectories. This feature can assist patients in understanding whether they are engaging the correct muscles during exertion or compensating with other muscles. Thus, our pipeline adds value to rehabilitation assistance.

In Figure 7a, we showcased the real-time performance of our proposed pipeline. For actions that are prone to misinterpretation, such as crossed legs (shown in Figure 7b), and for situations with obstructions (shown in Figure 7c), our pipeline demonstrates robust performance. These real-world test results affirm that the proposed pipeline is not only highly accurate but also practical and versatile.

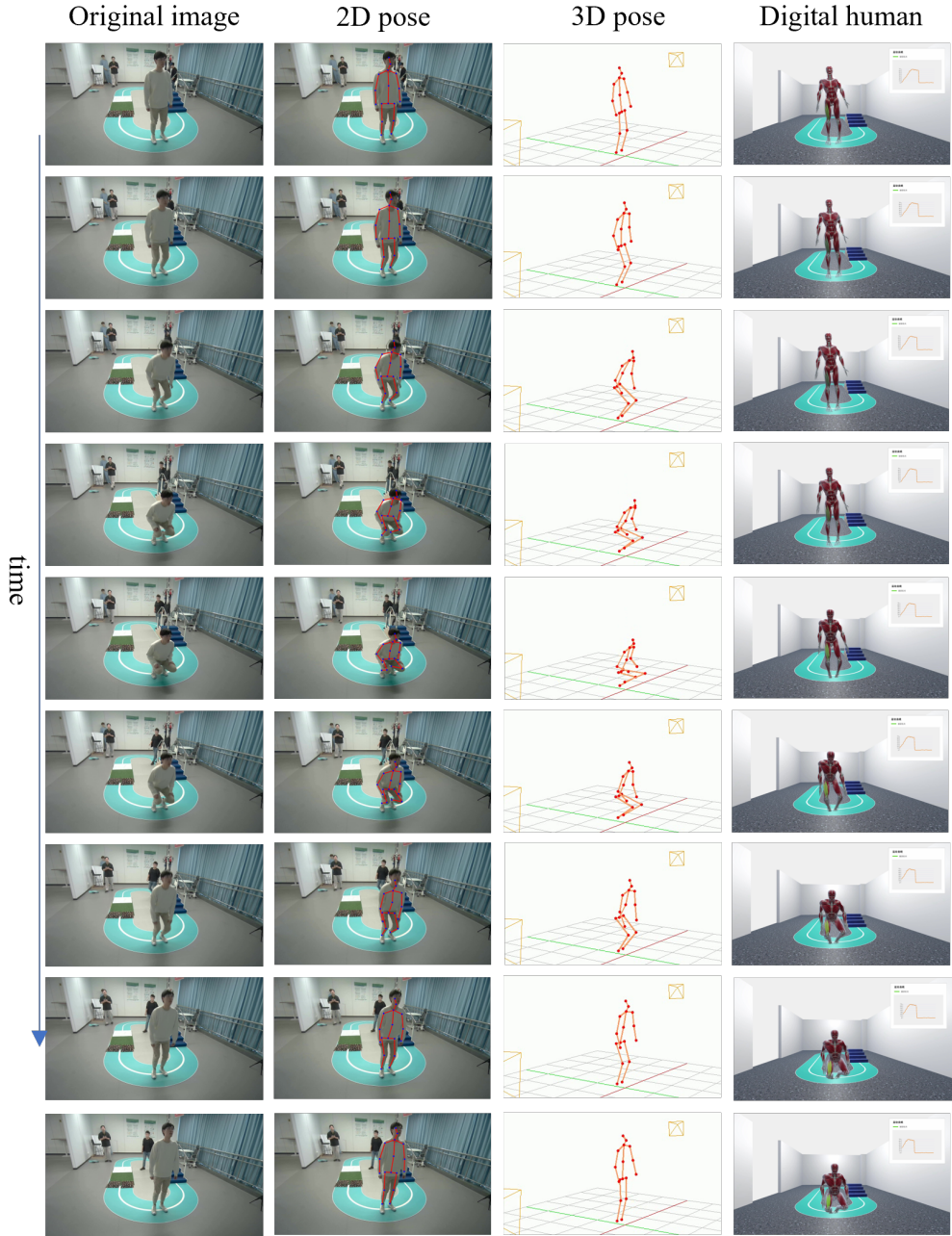


Figure 6 The visualization of input images (only 1 camera), 2D pose, 3D pose generated by our pipeline, and digital human with Color representation of stressed muscles.

5 Future works

While our pipeline has achieved commendable results in Real-life scenarios, there are still areas that require improvement. Our future research will primarily focus on:

Occlusion Issues. When a doctor or family member is assisting in training, occlusions are inevitable, which can be critical for image-based pose estimation, as shown in Figure 8. We plan to address this issue by utilizing a multi-camera collaboration, where the pipeline will automatically select the camera view that is not obstructed for pose estimation.

Video Processing. Currently, our pipeline processes each frame individually and then applies SmoothNet filtering. This

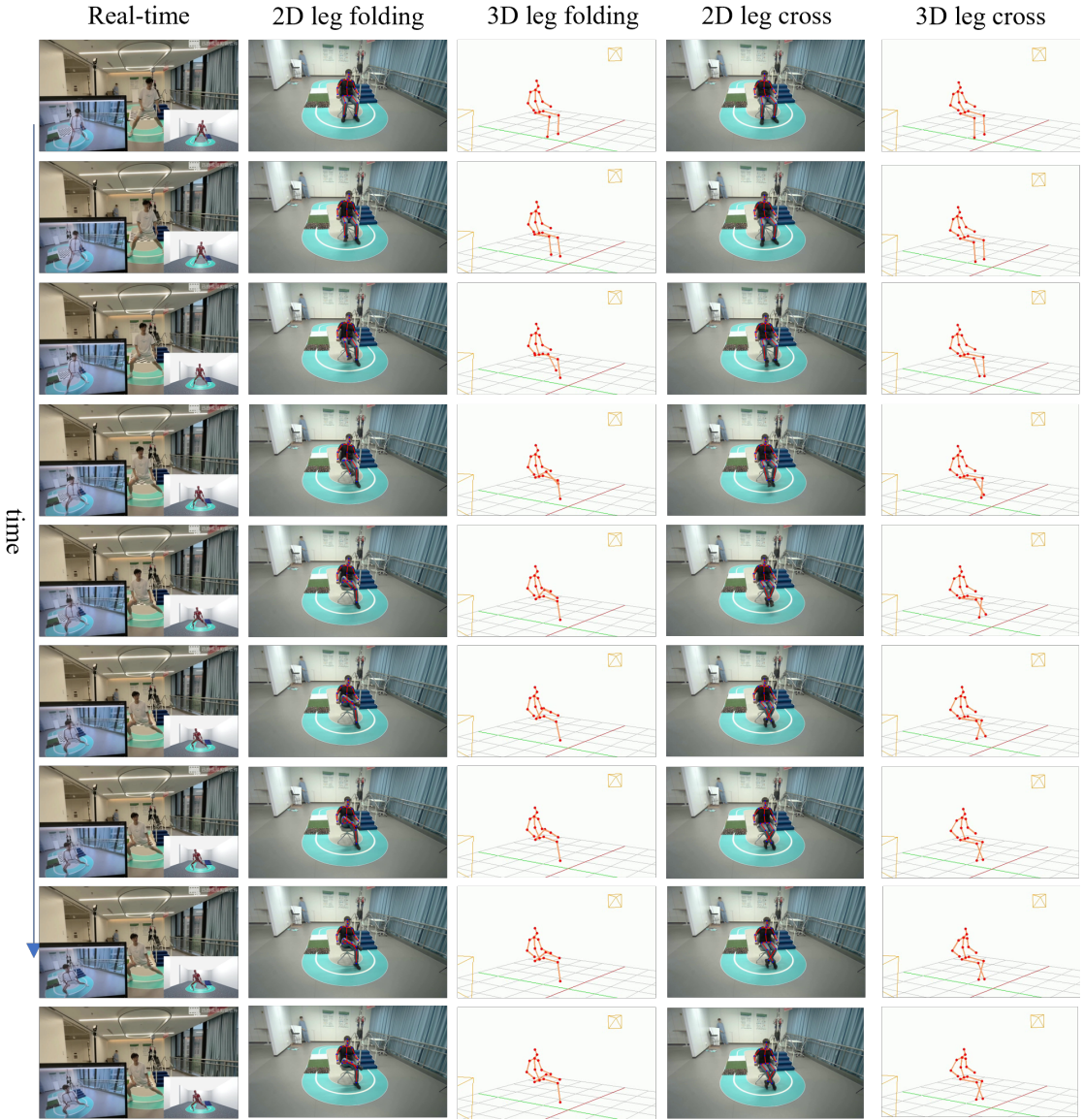


Figure 7 Real-time performance visualization, and 2D Pose and 3D Pose visualization in Leg Fold and Crossing cases.

does not fully leverage the temporal information in videos. Therefore, we will explore how to extract temporal features without compromising inference speed.

Patient-Specific Posture Prior. Since there is a significant difference between the postures of patients and healthy individuals, the prior information about patients’ behavior is very important. Hence, we will focus on data collection and training specific to patients to reinforce our pipeline.

Overall, our pipeline has performed exceedingly well for real-time applications, but we believe that further research in these directions will enhance its accuracy, efficiency, and applicability in medical rehabilitation scenarios.

6 Conclusion

We have proposed an end-to-end real-time 3D human pose recognition and motion analysis framework for rehabilitation training. This comprehensive pipeline integrates target detection, high-speed tracking, 2D/3D pose estimation, and temporal refinement via a modified SmoothNet, culminating in muscle stress quantification and digital human

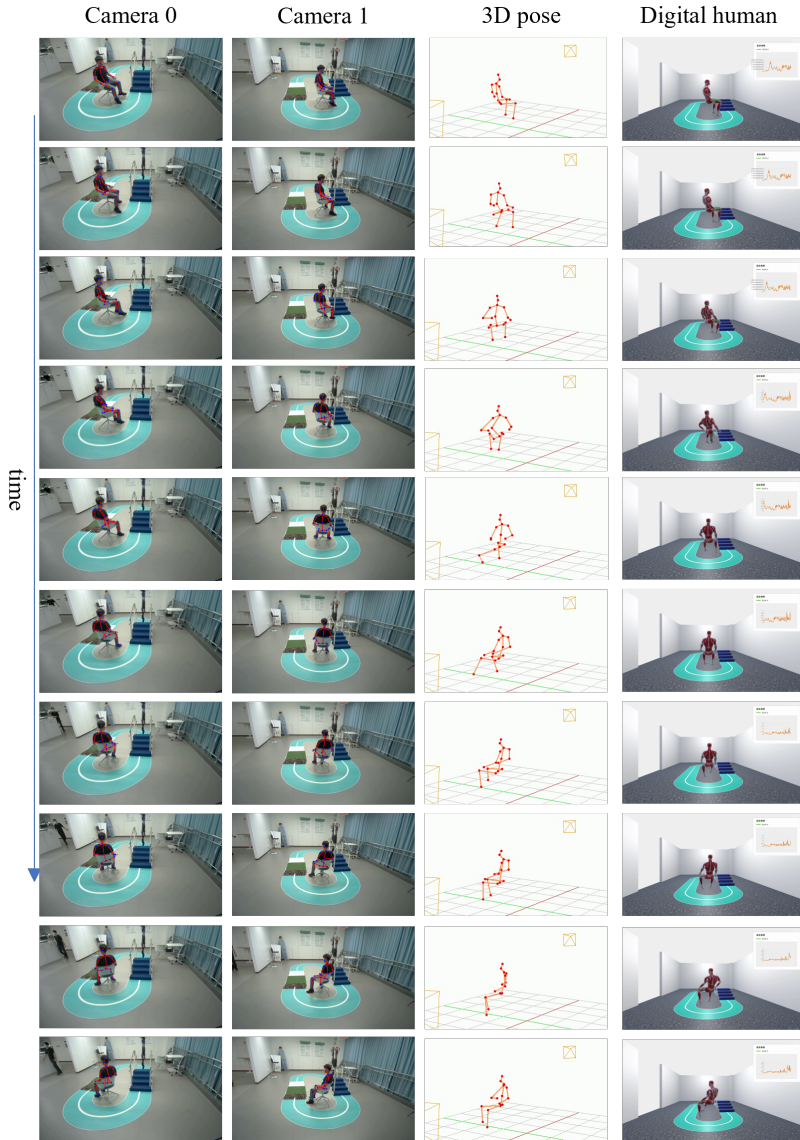


Figure 8 Visualization of occlusion situations by different cameras, and the 3D articulation points and digital humans they generate.

visualization. The proposed method not only achieves state-of-the-art accuracy on the Human3.6M dataset but also demonstrates exceptional computational efficiency suitable for real-time deployment. It provides patients and clinicians with a powerful tool for monitoring muscle engagement and ensuring exercise safety through immediate feedback. Beyond its technical contributions, this research holds significant social impact; by facilitating accessible home-based rehabilitation, it has the potential to reduce healthcare costs and alleviate the burden on clinical resources in an aging society. Future work will focus on further optimizing the system’s portability for mobile devices and conducting extensive clinical validations to support a wider range of recovery needs.

References

- [1] Andreas Aristidou and Joan Lasenby. Fabrik: A fast, iterative solver for the inverse kinematics problem. *Graphical Models*, 73(5):243–260, 2011.
- [2] Mohamed Bouri, Yves Stauffer, Carl Schmitt, Yves Allemand, Stany Gnement, Reymond Clavel, Patrick Metrailler, and Roland Brodard. The walktrainer: a robotic system for walking rehabilitation. In *2006 IEEE International Conference on Robotics and Biomimetics*, pages 1616–1621. IEEE, 2006.
- [3] Tianlang Chen, Chen Fang, Xiaohui Shen, Yiheng Zhu, Zhili Chen, and Jiebo Luo. Anatomy-aware 3d human pose estimation with bone-based pose decomposition. *IEEE Transactions on Circuits and Systems for Video Technology*, 32(1):198–209, 2021.
- [4] Swakshar Deb, Md Fokhrul Islam, Shafin Rahman, and Sejuti Rahman. Graph convolutional networks for assessment of physical rehabilitation exercises. *IEEE Transactions on Neural Systems and Rehabilitation Engineering*, 30:410–419, 2022.
- [5] Iñaki Díaz, Jorge Juan Gil, Emilio Sánchez, et al. Lower-limb robotic rehabilitation: literature review and challenges. *Journal of Robotics*, 2011, 2011.
- [6] Cheng-Yang Fu, Wei Liu, Ananth Ranga, Ambrish Tyagi, and Alexander C Berg. Dssd: Deconvolutional single shot detector. *arXiv preprint arXiv:1701.06659*, 2017.
- [7] Lynne V Gauthier, Chelsea Kane, Alexandra Borstad, Nancy Strahl, Gitendra Uswatte, Edward Taub, David Morris, Alli Hall, Melissa Arakelian, and Victor Mark. Video game rehabilitation for outpatient stroke (vigorous): protocol for a multi-center comparative effectiveness trial of in-home gamified constraint-induced movement therapy for rehabilitation of chronic upper extremity hemiparesis. *BMC neurology*, 17(1):1–18, 2017.
- [8] Ross Girshick. Fast r-cnn. In *Proceedings of the IEEE international conference on computer vision*, pages 1440–1448, 2015.
- [9] Yiwen Gu, Shreya Pandit, Elham Saraee, Timothy Nordahl, Terry Ellis, and Margrit Betke. Home-based physical therapy with an interactive computer vision system. In *Proceedings of the IEEE/CVF International Conference on Computer Vision Workshops*, pages 0–0, 2019.
- [10] Jianqiao Guo, Hongshi Huang, Yuanyuan Yu, Zixuan Liang, Jorge Ambrósio, Zhihua Zhao, Gexue Ren, and Yingfang Ao. Modeling muscle wrapping and mass flow using a mass-variable multibody formulation. *Multibody System Dynamics*, 49:315–336, 2020.
- [11] Jianqiao Guo, Wei Guo, and Gexue Ren. Embodiment of intra-abdominal pressure in a flexible multibody model of the trunk and the spinal unloading effects during static lifting tasks. *Biomechanics and Modeling in Mechanobiology*, 20(4):1599–1626, 2021.
- [12] Kaiming He, Georgia Gkioxari, Piotr Dollár, and Ross Girshick. Mask r-cnn. In *Proceedings of the IEEE international conference on computer vision*, pages 2961–2969, 2017.
- [13] Catalin Ionescu, Dragos Papava, Vlad Olaru, and Cristian Sminchisescu. Human3. 6m: Large scale datasets and predictive methods for 3d human sensing in natural environments. *IEEE transactions on pattern analysis and machine intelligence*, 36(7):1325–1339, 2013.
- [14] Karim Iskakov, Egor Burkov, Victor Lempitsky, and Yury Malkov. Learnable triangulation of human pose. In *Proceedings of the IEEE/CVF international conference on computer vision*, pages 7718–7727, 2019.
- [15] Sašo Jezernik, Gery Colombo, Thierry Keller, Hansruedi Frueh, and Manfred Morari. Robotic orthosis lokomat: A rehabilitation and research tool. *Neuromodulation: Technology at the neural interface*, 6(2):108–115, 2003.
- [16] Ravi Komatireddy, Anang Chokshi, Jeanna Basnett, Michael Casale, Daniel Goble, and Tiffany Shubert. Quality and quantity of rehabilitation exercises delivered by a 3-d motion controlled camera: A pilot study. *International journal of physical medicine & rehabilitation*, 2(4), 2014.
- [17] Wenhao Li, Hong Liu, Hao Tang, Pichao Wang, and Luc Van Gool. Mhformer: Multi-hypothesis transformer for 3d human pose estimation. In *Proceedings of the IEEE/CVF Conference on Computer Vision and Pattern Recognition*, pages 13147–13156, 2022.
- [18] Yalin Liao, Aleksandar Vakanski, and Min Xian. A deep learning framework for assessing physical rehabilitation exercises. *IEEE Transactions on Neural Systems and Rehabilitation Engineering*, 28(2):468–477, 2020. doi: 10.1109/TNSRE.2020.2966249.
- [19] Tsung-Yi Lin, Piotr Dollár, Ross Girshick, Kaiming He, Bharath Hariharan, and Serge Belongie. Feature pyramid networks for object detection. In *Proceedings of the IEEE conference on computer vision and pattern recognition*, pages 2117–2125, 2017.

[20] Mandy Lu, Kathleen Poston, Adolf Pfefferbaum, Edith V Sullivan, Li Fei-Fei, Kilian M Pohl, Juan Carlos Niebles, and Ehsan Adeli. Vision-based estimation of mds-updrs gait scores for assessing parkinson's disease motor severity. In *Medical Image Computing and Computer Assisted Intervention–MICCAI 2020: 23rd International Conference, Lima, Peru, October 4–8, 2020, Proceedings, Part III 23*, pages 637–647. Springer, 2020.

[21] Steven R Machlin, Julia Chevan, William W Yu, and Marc W Zodet. Determinants of utilization and expenditures for episodes of ambulatory physical therapy among adults. *Physical therapy*, 91(7):1018–1029, 2011.

[22] Paweł Maciejasz, Jörg Eschweiler, Kurt Gerlach-Hahn, Arne Jansen-Troy, and Steffen Leonhardt. A survey on robotic devices for upper limb rehabilitation. *Journal of neuroengineering and rehabilitation*, 11(1):1–29, 2014.

[23] Alejandro Newell, Kaiyu Yang, and Jia Deng. Stacked hourglass networks for human pose estimation. In *Computer Vision–ECCV 2016: 14th European Conference, Amsterdam, The Netherlands, October 11–14, 2016, Proceedings, Part VIII 14*, pages 483–499. Springer, 2016.

[24] Dario Pavillo, Christoph Feichtenhofer, David Grangier, and Michael Auli. 3d human pose estimation in video with temporal convolutions and semi-supervised training. In *Proceedings of the IEEE/CVF conference on computer vision and pattern recognition*, pages 7753–7762, 2019.

[25] John Rasmussen, Michael Damsgaard, and Michael Voigt. Muscle recruitment by the min/max criterion—a comparative numerical study. *Journal of biomechanics*, 34(3):409–415, 2001.

[26] Reza Sharif Razavian, Naser Mehrabi, and John McPhee. A neuronal model of central pattern generator to account for natural motion variation. *Journal of Computational and Nonlinear Dynamics*, 11(2):021007, 2016.

[27] Swithin S Razu and Trent M Guess. Electromyography-driven forward dynamics simulation to estimate in vivo joint contact forces during normal, smooth, and bouncy gaits. *Journal of Biomechanical Engineering*, 140(7):071012, 2018.

[28] Shaoqing Ren, Kaiming He, Ross Girshick, and Jian Sun. Faster r-cnn: Towards real-time object detection with region proposal networks. *Advances in neural information processing systems*, 28, 2015.

[29] Zhiqiang Shen, Zhuang Liu, Jianguo Li, Yu-Gang Jiang, Yurong Chen, and Xiangyang Xue. Dsod: Learning deeply supervised object detectors from scratch. In *Proceedings of the IEEE international conference on computer vision*, pages 1919–1927, 2017.

[30] MPT Silva and JAC Ambrósio. Kinematic data consistency in the inverse dynamic analysis of biomechanical systems. *Multibody System Dynamics*, 8:219–239, 2002.

[31] Ke Sun, Bin Xiao, Dong Liu, and Jingdong Wang. Deep high-resolution representation learning for human pose estimation. In *Proceedings of the IEEE/CVF conference on computer vision and pattern recognition*, pages 5693–5703, 2019.

[32] Xiao Sun, Jiaxiang Shang, Shuang Liang, and Yichen Wei. Compositional human pose regression. In *Proceedings of the IEEE international conference on computer vision*, pages 2602–2611, 2017.

[33] Juan Terven and Diana Cordova-Esparza. A comprehensive review of yolo: From yolov1 to yolov8 and beyond. *arXiv preprint arXiv:2304.00501*, 2023.

[34] Alexander Toshev and Christian Szegedy. Deeppose: Human pose estimation via deep neural networks. In *Proceedings of the IEEE conference on computer vision and pattern recognition*, pages 1653–1660, 2014.

[35] Hanyue Tu, Chunyu Wang, and Wenjun Zeng. Voxelpose: Towards multi-camera 3d human pose estimation in wild environment. In *Computer Vision–ECCV 2020: 16th European Conference, Glasgow, UK, August 23–28, 2020, Proceedings, Part I 16*, pages 197–212. Springer, 2020.

[36] Xinyue Wang, Jianqiao Guo, and Qiang Tian. A forward-inverse dynamics modeling framework for human musculoskeletal multibody system. *Acta Mechanica Sinica*, 38(11):522140, 2022.

[37] Yifan Wang, Jian Zhao, Zhaoxin Fan, Xin Zhang, Xuecheng Wu, Yudian Zhang, Lei Jin, Xinyue Li, Gang Wang, Mengxi Jia, et al. Jtd-uav: Mllm-enhanced joint tracking and description framework for anti-uav systems. In *Proceedings of the Computer Vision and Pattern Recognition Conference*, pages 1633–1644, 2025.

[38] Shih-En Wei, Varun Ramakrishna, Takeo Kanade, and Yaser Sheikh. Convolutional pose machines. In *Proceedings of the IEEE conference on Computer Vision and Pattern Recognition*, pages 4724–4732, 2016.

[39] Tian-Hao Wu, Tong-Wen Wang, and Ya-Qi Liu. Real-time vehicle and distance detection based on improved yolo v5 network. In *2021 3rd World Symposium on Artificial Intelligence (WSAI)*, pages 24–28. IEEE, 2021.

[40] Xuecheng Wu, Jiaxing Liu, Danlei Huang, Xiaoyu Li, Yifan Wang, Chen Chen, Liya Ma, Xuezhi Cao, and Junxiao Xue. Vic-bench: Benchmarking visual-interleaved chain-of-thought capability in mllms with free-style intermediate state representations. *arXiv preprint arXiv:2505.14404*, 2025.

[41] Xuecheng Wu, Heli Sun, Yifan Wang, Jiayu Nie, Jie Zhang, Yabing Wang, Junxiao Xue, and Liang He. Avf-mae++: Scaling affective video facial masked autoencoders via efficient audio-visual self-supervised learning. In *Proceedings of the Computer Vision and Pattern Recognition Conference*, pages 9142–9153, 2025.

[42] Xuecheng Wu, Heli Sun, Junxiao Xue, Jiayu Nie, Xiangyan Kong, Ruofan Zhai, Danlei Huang, and Liang He. Towards emotion analysis in short-form videos: A large-scale dataset and baseline. In *Proceedings of the 2025 International Conference on Multimedia Retrieval*, pages 1497–1506, 2025.

[43] Xuecheng Wu, Junxiao Xue, Xinyi Yin, Yunyun Shi, Liangyu Fu, Danlei Huang, Yifan Wang, Jia Zhang, Jiayu Nie, and Jun Wang. Scalable audiovisual masked autoencoders for efficient affective video facial analysis. *Intelligent Computing*, 2025.

[44] Hang Ye, Wentao Zhu, Chunyu Wang, Ruijie Wu, and Yizhou Wang. Faster voxelpose: Real-time 3d human pose estimation by orthographic projection. In *European Conference on Computer Vision*, pages 142–159. Springer, 2022.

[45] Ailing Zeng, Lei Yang, Xuan Ju, Jiefeng Li, Jianyi Wang, and Qiang Xu. Smoothnet: A plug-and-play network for refining human poses in videos. In *European Conference on Computer Vision*, pages 625–642. Springer, 2022.

[46] Jianfeng Zhang, Yujun Cai, Shuicheng Yan, Jiashi Feng, et al. Direct multi-view multi-person 3d pose estimation. *Advances in Neural Information Processing Systems*, 34:13153–13164, 2021.

[47] Zhe Zhang, Chunyu Wang, Weichao Qiu, Wenhui Qin, and Wenjun Zeng. Adafuse: Adaptive multiview fusion for accurate human pose estimation in the wild. *International Journal of Computer Vision*, 129:703–718, 2021.

[48] Qitao Zhao, Ce Zheng, Mengyuan Liu, Pichao Wang, and Chen Chen. Poseformerv2: Exploring frequency domain for efficient and robust 3d human pose estimation. In *Proceedings of the IEEE/CVF Conference on Computer Vision and Pattern Recognition*, pages 8877–8886, 2023.

[49] Zhong-Qiu Zhao, Peng Zheng, Shou-tao Xu, and Xindong Wu. Object detection with deep learning: A review. *IEEE transactions on neural networks and learning systems*, 30(11):3212–3232, 2019.

[50] Ce Zheng, Wenhan Wu, Chen Chen, Taojiannan Yang, Sijie Zhu, Ju Shen, Nasser Kehtarnavaz, and Mubarak Shah. Deep learning-based human pose estimation: A survey. *ACM Computing Surveys*, 56(1):1–37, 2023.